Jet energy loss, photon production, and photon-hadron correlations at energies available at the BNL Relativistic Heavy Ion Collider (RHIC)

Guang-You Qin,[1] Jörg Ruppert,[2] Charles Gale,[2] Sangyong Jeon,[2] and Guy D. Moore[2,3]
[1]*Department of Physics, The Ohio State University, Columbus, Ohio, 43210, USA*
[2]*Department of Physics, McGill University, Montreal, Quebec, H3A 2T8, Canada*
[3]*Universidad Autonoma de Madrid, E-28049 Madrid, Spain*
(Received 15 July 2009; published 16 November 2009)

Jet energy loss, photon production, and photon-hadron correlations are studied together at high transverse momentum in relativistic heavy-ion collisions at Relativistic Heavy Ion Collider (RHIC) energies. The modification of hard jets traversing a hot and dense nuclear medium is evaluated by consistently taking into account induced gluon radiation and elastic collisions. The production of high-transverse-momentum photons in Au + Au collisions at RHIC is calculated by incorporating a complete set of photon-production channels. Comparison with experimental photon production and photon-hadron correlation data is performed, using a $(3+1)$-dimensional relativistic hydrodynamic description of the thermalized medium created in these collisions. Our results demonstrate that the interaction between the hard jets and the soft medium is important for the study of photon production and of photon-hadron correlation at RHIC.

DOI: 10.1103/PhysRevC.80.054909 PACS number(s): 25.75.Cj, 25.75.Gz, 25.75.Nq

I. INTRODUCTION

Hard processes are regarded as good tools for the tomographic study of relativistic heavy-ion collisions and of the quark-gluon plasma: The energetic probes are created in the early stage of the collisions and can therefore access the space-time history of the transient hot and dense nuclear medium created in these collisions. Large transverse-momentum partons have been identified as especially useful because they interact directly with the nuclear medium and will lose energy in the process. The partonic jets that emerge will fragment into the hadrons that are observed in the detectors. Experiments at the Relativistic Heavy Ion Collider (RHIC) at Brookhaven National Laboratory (BNL) have indeed shown that high-p_T hadrons in central $A+A$ collisions are significantly suppressed in comparison with those in binary-scaled $p+p$ interactions [1–3]. Those results are commonly referred to as "jet quenching."

A lot of effort has been devoted to describe the energy loss experienced by the color charges inside the hot, strongly interacting matter. Gluon bremsstrahlung with the Landau-Pomeranchuk-Migdal (LPM) [4] effect has been proposed as the dominant mechanism for the jet-quenching process, and different theoretical formalisms have been elaborated to describe the hard parton energy loss [5–15]. Several of these bremsstrahlung calculations were compared against each other [16–19], using a relativistic ideal $(3+1)$-dimensional hydrodynamical simulation of the strongly interacting medium [20]. This implementation improved on earlier attempts relying on simple schematic models by building on a detailed and realistic description of the time evolution. Another potentially important energy loss mechanism for high-p_T color charges is provided by scattering off thermal partons in binary elastic collisions. Estimations of the relative magnitude of collisional versus radiative energy loss have also been performed in several different approaches and scenarios [21–28]. In Ref. [29], a study of radiative and collisional energy loss was carried out in a given single approach (AMY [13–15]). Note that the collisional energy loss was further improved on in Ref. [30].

Complementary to hadronic species, photons represent another set of promising observables with the potential of probing the quark-gluon plasma (see, for example, [31] and references therein). Because they carry no color charge, once produced, they will essentially escape from the collision zone without further interaction with the surrounding nuclear medium, reflecting directly local medium properties. However, the experimental observation of produced photons in high-energy nuclear collisions involves the entire evolution of the collision, together with a variety of sources. Considering that the background contribution from meson decay may in principle be experimentally subtracted, theoretical studies need to include photons produced in the early collisions, those involving jet-medium interactions during jet propagation in the medium [32], and those from fragmentation of the surviving jets after their escape from the medium. In Refs. [33,34], the calculation of photon production from nuclear collisions at RHIC with those different photon sources has been done by first employing a $(1+1)$-dimensional Bjorken evolution model and then $(2+1)$-dimensional relativistic hydrodynamics.

These calculations, and others, have given rise to the hope that the "tomography" of the hot and dense core of the nuclear medium created in relativistic heavy-ion collisions may be put on a firm quantitative footing.

In what concerns hadrons, several quantities have been put forward as "tomographic variables." One of those is the nuclear modification factor R_{AA} that is inferred from the measurement of single-particle inclusive p_T spectra. It is defined as the ratio of the hadron yield in $A+A$ collisions to that in binary-scaled $p+p$ interactions. Because the single-particle spectrum is a convolution of the jet production cross section and jet fragmentation functions, the suppression of the produced hadrons at a fixed p_T involves jets with a wide range of initial transverse energies; for details see Refs. [16,29]. In retrospect, it is therefore not particularly surprising that a wide variety of

energy loss conjectures that differ significantly in the predicted energy loss mechanism can reproduce the measured R_{AA} in central Au + Au collisions at $\sqrt{s} = 200A$ GeV at RHIC given the present experimental errors for central collisions. In that sense, the tomographic usefulness of R_{AA} in central collisions has become rather questionable [35]. There have been several suggestions to improve the situation. One is to consider a more differential observable and study R_{AA} in noncentral collisions as a function of the azimuth and p_T [36]. This effectively corresponds to studying an average over different paths of partons as they traverse the expanding medium, which is no longer rotationally invariant in the transverse plane. In Ref. [16], R_{AA} was also studied as a function of p_T in central and noncentral collisions at mid- and forward rapidities. Although this does not restrict the initial jets' energies or initial vertices, it allows for a different averaging over the medium than in central collisions and can thus provide us with additional information.

Another road to improvement consists of considering many-body variables, e.g., to study the production of high-p_T hadrons correlated with other high-p_T particles. One motivation is that the correlation between the trigger particle and the measured hadrons will constrain the initial energy distribution of the parton that fragments into the hadrons more tightly than single-particle measurements. One such suggested trigger is a hadron, see, e.g., Ref. [37]. Note, however, that choosing a specific p_T for the trigger hadron on the "near side" still does not strictly pin down the energy of the "away-side" partons. The trigger hadron is produced by fragmentation of partons that have also traversed the medium and lost energy. Therefore, a specific trigger bias is introduced into the away-side parton distribution and initial vertex distribution. This effect has been explored in Ref. [37], where a detailed analysis of the initial vertex density and conditional probability distribution $P(p_T)$ of away-side partons for di-hadron correlations was presented in the Baier-Dokshitzer-Mueller-Peigne-Schiff (BDMPS) framework of energy loss [5] by gluon bremsstrahlung. There it was shown that the yield of hadrons per trigger hadron was sensitive to the specific assumptions about the evolution model for dihadron correlations, while it was not for R_{AA}.

Another promising trigger is a high-p_T photon: One studies jet quenching by measuring the p_T distribution of charged hadrons in the opposite direction of a trigger direct photon [38,39]. Direct photons are predominantly produced from hard collisions in the early stage of relativistic nuclear collisions. Assuming that a high-p_T direct photon from these processes can be used as a trigger of the away-side hadron, the transverse energy of the initial away-side parton before energy loss can then be deduced (up to corrections at next to leading order in α_s). Thus, direct photons can provide a calibrated probe for the study of the properties of high-energy-density QCD. This kind of trigger does not introduce a vertex bias and therefore weighs all vertices according to the nuclear overlap function, and it strongly restricts the initial away-side partons' energy to a monoenergetic source. Given this restriction of the initial jet's transverse energy, the expected tomographic capabilities of photon-tagged jet correlation measurements are much higher than those of R_{AA}. It has been shown in Ref. [35] that while different schematic conjectures of jet energy losses could not be discriminated by R_{AA} in central collisions at midrapidity, they gave clearly different predictions for γ-hadron correlations. Some other studies have also been performed along this direction [40–42].

However, jet-photon correlation calculations need to go beyond direct photons and to include the other important and known electromagnetic sources such as fragmentation and jet-medium interaction. As the initial away-side partonic jets in these processes could have larger transverse energies than the near-side trigger photon, photons produced from those processes might have significant contribution to the correlations between final photons and hadrons. In this work, we consider these possibilities and incorporate a complete set of high-p_T photon-production channels and study their relative contributions to the correlations between back-to-back photons and hadrons.

In Ref. [29], we have presented a consistent calculation of both collisional and radiative energy loss in the same formalism. There it was applied to calculate the nuclear modification factor R_{AA} of neutral pions in heavy-ion collisions at RHIC for different centralities at midrapidity. Here, we continue and extend this effort by studying the effect of jet-medium interaction on the photon production as well as on correlated back-to-back hard photons and hadrons in high-energy nuclear collisions. We employ the formalism developed in Ref. [29] to account consistently for collisional and radiative energy loss of the leading hard parton while it traverses the surrounding soft nuclear matter, modeled by (3 + 1)-dimensional hydrodynamics [20].

This article is organized as follows: the next two sections describe our approach to jet energy loss and to photon production. Then, photon-hadron correlations are treated, and comparisons with experimental results obtained at RHIC by the PHENIX and STAR Collaborations are performed.

II. JET ENERGY LOSS

In our approach, hard jets (quarks and gluons) evolve in the soft nuclear medium according to a set of Fokker-Planck-type rate equations for their momentum distributions $P(E,t) = dN(E,t)/dE$. The generic form of these rate equations can be written as follows [33,43],

$$\frac{dP_j(E,t)}{dt} = \sum_{ab}\int d\omega \left[P_a(E+\omega,t)\frac{d\Gamma_{a\to j}(E+\omega,\omega)}{d\omega dt} - P_j(E,t)\frac{d\Gamma_{j\to b}(E,\omega)}{d\omega dt}\right], \quad (1)$$

where $d\Gamma_{j\to a}(E,\omega)/d\omega dt$ is the transition rate for the partonic process $j \to a$, with E the initial jet energy and ω the energy lost in the process. The $\omega < 0$ part of the integration accounts for the contribution from the energy-gain channels. The radiative and collisional parts of the transition rates have been extensively discussed in Ref. [16,29,44].

The initial jet momentum profiles may be computed from perturbative QCD calculations [45],

$$\frac{d\sigma_{AB\to jX}}{d^2p_T^j dy} = K_{\rm jet}\sum_{abd}\int dx_a G_{a/A}(x_a, Q)G_{b/B}(x_b, Q) \times \frac{1}{\pi}\frac{2x_a x_b}{2x_a - x_T^j e^y}\frac{d\sigma_{ab\to jd}}{dt}, \quad (2)$$

with $x_T^j = 2p_T^j/\sqrt{s_{NN}}$, where $\sqrt{s_{NN}}$ is the center-of-mass energy. In the above equation, $G_{a/A}(x_a, Q)$ is the distribution function of parton a with momentum fraction x_a in the nucleus A at factorization scale Q, taken from CTEQ5 [46], including nuclear shadowing effects from EKS98 [47]. The distribution $d\sigma/dt$ is the leading-order QCD differential cross section with $K_{\rm jet}$ accounting for next-to-leading order (NLO) corrections. It is fixed following Ref. [48] by reproducing the experimental measurement of the inclusive π^0 cross section at high-p_T in in $p+p$ collisions at $\sqrt{s_{NN}} = 200$ GeV (see Fig. 1 in Ref. [16]). The $K_{\rm jet}$ factor is found to be 2.8 when the renormalization scale and the factorization scale are taken to be the transverse momentum of the initial jets, and the fragmentation scale is taken to be the transverse momentum of produced hadrons.

To obtain the final high-p_T hadron spectra in Au + Au collisions at RHIC, the energy loss of partonic jets in the nuclear medium must be taken into account. This is performed by calculating the medium-modified fragmentation function $\tilde{D}_{h/j}(z, \vec{r}_\perp, \phi)$ for a single partonic jet,

$$\tilde{D}_{h/j}(z, \vec{r}_\perp, \phi) = \sum_{j'}\int dp_{j'}\frac{z'}{z}D_{h/j'}(z')P(p_{j'}|p_j, \vec{r}_\perp, \phi), \quad (3)$$

where $z = p_h/p_j$ and $z' = p_h/p_{j'}$ are two momentum fractions with p_h the hadron momentum and $p_j(p_{j'})$ the initial (final) jet momentum; $D_{h/j}(z)$ is the vacuum fragmentation function, taken from the KKP parametrization [49]. In the above equation, the probability function $P(p_{j'}|p_j, \vec{r}_\perp, \phi)$ is obtained by solving Eq. (1), representing the probability of obtaining a jet j' with momentum $p_{j'}$ from a given jet j with momentum p_j. This depends on the path taken by the parton and the medium profile along that path, which in turn depends on the original location of the jet, $\vec{r}_\perp$, and on its propagation angle ϕ with respect to the reaction plane. Therefore, one must convolve the above expression over all transverse positions and directions to obtain the final hadron spectra:

$$\frac{d\sigma_{AB\to hX}}{d^2p_T^h dy} = \frac{1}{2\pi}\int d^2\vec{r}_\perp \mathcal{P}_{AB}(b, \vec{r}_\perp) \times \sum_j \int \frac{dz}{z^2}\tilde{D}_{h/j}(z, \vec{r}_\perp, \phi)\frac{d\sigma_{AB\to jX}}{d^2p_T^j dy}, \quad (4)$$

where $\mathcal{P}_{AB}(b, \vec{r}_\perp)$ is the probability distribution of initial hard jets in the transverse position $\vec{r}_\perp$, which is determined from the overlap geometry between two nuclei in the transverse plane of the collision zone. For A + B collisions at impact parameter b,

$$\mathcal{P}_{AB}(b, \vec{r}_\perp) = \frac{T_A(\vec{r}_\perp + \vec{b}/2)T_B(\vec{r}_\perp - \vec{b}/2)}{T_{AB}(b)}, \quad (5)$$

where $T_A(\vec{r}_\perp) = \int dz\rho_A(\vec{r}_\perp, z)$ is the nuclear thickness function and $T_{AB}(b) = \int d^2r_\perp T_A(\vec{r}_\perp)T_B(\vec{r}_\perp + \vec{b})$ is the nuclear overlap function. A Woods-Saxon form for the nuclear density function $\rho(\vec{r}_\perp, z) = \rho_0/[1 + \exp(\frac{r-R}{d})]$ is used, and the values of the parameters $R = 6.38$ fm and $d = 0.535$ fm are taken from Ref. [50].

Putting all of the above together, one obtains the total yield of hadrons produced in relativistic nuclear collisions,

$$\frac{dN_{AB}^h(b)}{d^2p_T^h dy} = \frac{N_{\rm coll}(b)}{\sigma_{NN}}\frac{d\sigma_{AB\to hX}}{d^2p_T^h dy}, \quad (6)$$

where $N_{\rm coll}$ is the number of binary collisions and σ_{NN} is the inelastic cross section of elementary nucleon-nucleon collisions. Finally, the nuclear modification factor R_{AA} is defined as the ratio of the hadron yield in $A+A$ collisions to that in $p+p$ interactions scaled by the number of binary collisions,

$$R_{AA}^h = \frac{1}{N_{\rm coll}(b)}\frac{dN_{AA}^h(b)/d^2p_T^h dy}{dN_{pp}^h/d^2p_T^h dy}. \quad (7)$$

III. PHOTON PRODUCTION

As mentioned, there are several sources of high-p_T photons in relativistic nuclear collisions. The most important are direct photons, fragmentation photons, and jet-medium photons (bremsstrahlung photons and conversion photons). The thermal photon emission arising from the partonic medium and later hadronic phase makes a negligible contribution in the high-p_T regime and thus is excluded from consideration in the present calculation.

Direct photons are predominantly produced from early hard collisions between partons from the initial nuclei, via quark-antiquark annihilation ($q + \bar{q} \to g + \gamma$) and quark-gluon Compton scattering [$q(\bar{q}) + g \to q(\bar{q}) + \gamma$]. The inclusive direct photon cross section may be calculated from Eq. (2) by applying the corresponding partonic processes for photon production,

$$\frac{d\sigma_{AB\to\gamma X}^{\rm direct}}{d^2p_T^\gamma dy} = K_\gamma\sum_{abd}\int dx_a G_{a/A}(x_a, Q)G_{b/B}(x_b, Q) \times \frac{1}{\pi}\frac{2x_a x_b}{2x_a - x_T^\gamma e^y}\frac{d\sigma_{ab\to\gamma d}}{dt}, \quad (8)$$

with $x_T^\gamma = 2p_T^\gamma/\sqrt{s_{NN}}$. The factor K_γ is a function of the photon's transverse momentum and is deduced by performing an NLO calculation of photon production in $p+p$ collisions [51–53], in which all scales are set to be the photon transverse momentum. Note that by directly fitting to the photon data in $p+p$ collisions, one obtains the values for K_γ close to these extracted from NLO calculation.

Fragmentation photons are produced by the surviving high-energy jets after their passing through the hot and dense nuclear medium. The calculation of fragmentation photon spectra is similar to that of the high-p_T hadron production described in the last section. We may also define a medium-modified photon fragmentation function $\tilde{D}_{\gamma/j}(z, \vec{r}_\perp, \phi)$ as in Eq. (3). Then the final expression for the fragmentation photon cross

section can be written as

$$\frac{d\sigma^{\rm frag}_{AB\to\gamma X}}{d^2p_T^\gamma dy} = \frac{1}{2\pi}\int d^2\vec{r}_\perp \mathcal{P}_{AB}(\vec{r}_\perp) \times \sum_j \int \frac{dz}{z^2}\tilde{D}_{\gamma/j}(z,\vec{r}_\perp,\phi)\frac{d\sigma_{AB\to jX}}{d^2p_T^j dy}. \quad (9)$$

where the vacuum fragmentation functions of quarks and gluons into real photons are taken from Ref. [54] with the fragmentation scale set to be photon transverse momenta and $d\sigma_{AB\to jX}$ is the initial jet spectra from Eq. (2). The same value for $K_{\rm jet}$ is used here and in jet-medium photon calculation; note this choice is not unique.

Jet-medium photons are produced by jet-medium interactions during the passage of jets through the hot nuclear medium. These include induced photon radiation (bremsstrahlung photons) and direct conversion from the high-energy jets (conversion photons). It has been shown that those two processes are important for the understanding of experimental data for photon production in Au + Au collisions at RHIC [32–34].

To incorporate the photons directly produced from jet-medium interaction, we may add to the set of evolution equations shown in Eq. (1) an additional evolution equation for photons,

$$\frac{dP_\gamma^{\rm JM}(E,t)}{dt} = \int d\omega P_{q\bar{q}}(E+\omega,t)\frac{d\Gamma^{\rm JM}_{q\to\gamma}(E+\omega,\omega)}{d\omega dt}, \quad (10)$$

where $d\Gamma^{\rm JM}_{q\to\gamma}/d\omega dt = d\Gamma^{\rm brem}_{q\to\gamma}/d\omega dt + d\Gamma^{\rm conv}_{q\to\gamma}/d\omega dt$. The transition rates $d\Gamma^{\rm brem}_{q\to\gamma}/d\omega dt$ for photon bremsstrahlung processes are similar to gluon bremsstrahlung processes and are extensively discussed in Refs. [13–15]. And the transition rates $d\Gamma^{\rm conv}_{q\to\gamma}/d\omega dt$ for binary jet-photon conversion processes may be inferred from the photon emission rates for those processes [55],

$$\frac{d\Gamma^{\rm conv}_{q\to\gamma}(E,\omega)}{d\omega dt} = \sum_f \left(\frac{e_f}{e}\right)^2 \frac{2\pi\alpha_e\alpha_s T^2}{3E} \times \left[\frac{1}{2}\ln\frac{ET}{m_q^2} + C_{2\to2}(E/T)\right]\delta(\omega), \quad (11)$$

where $m_q^2 = g_s^2T^2/6$ is the thermal quark mass and $C_{2\to2} \approx -0.36149$ in the limit of $E \gg T$ [15,56,57]. The function $\delta(\omega)$ represents the fact that the produced photon has essentially the same energy as the incoming quarks (or antiquarks) in the jet-photon conversion processes.

IV. PHOTON-HADRON CORRELATIONS

In this section, we present the calculation of the correlation between back-to-back hard photons and hadrons. The associated hadrons are produced from the fragmentation of surviving jets after their passing through the nuclear medium, while the trigger photons may come from various sources as has been discussed in the previous section. Therefore, the photon–hadron correlation will depend on the jet-photon correlation at the production vertex as well as on the energy loss of the jets during their propagation in the medium.

In correlation studies, one of the commonly exploited observables is the yield per trigger, which is the momentum distribution of produced hadrons on the away side, given a trigger photon of momentum p_T^γ in the near side. Following Ref. [58], one may write

$$P(p_T^h|p_T^\gamma) = \frac{P(p_T^h, p_T^\gamma)}{P(p_T^\gamma)}, \quad (12)$$

where $P(p_T^\gamma) = 1/\sigma_{\rm tot}\int dy_\gamma d\sigma_\gamma/dy_\gamma dp_T^\gamma$ represents the single-particle p_T distribution and $P(p_T^\gamma, p_T^h) = 1/\sigma_{\rm tot}\int dy_\gamma dy_h d\sigma_{\gamma+h}/dy_\gamma dy_h dp_T^\gamma dp_T^h$ is the $\gamma - h$ pair p_T distribution.

The trigger photon and the associated hadron are produced from a pair of back-to-back partons. Assuming no correlation between the individual evolutions of two partonic jets once they are produced, we may write down the expressions of these two distributions as follows

$$P_f(p_T^\gamma) = \int\frac{d\phi}{2\pi}\int d^2\vec{r}_\perp\mathcal{P}_{AB}(\vec{r}_\perp) \times \sum_j\int dp_T^j P_i(p_T^j)P(p_T^\gamma|p_T^j,\vec{r}_\perp,\phi),$$

$$P_f(p_T^h, p_T^\gamma) = \int\frac{d\phi}{2\pi}\int d^2\vec{r}_\perp\mathcal{P}_{AB}(\vec{r}_\perp) \times\sum_{jj'}\int dp_T^j dp_T^{j'} P_i(p_T^j, p_T^{j'})P(p_T^\gamma|p_T^j,\vec{r}_\perp,\phi) \times P(p_T^h|p_T^{j'},\vec{r}_\perp,\pi+\phi). \quad (13)$$

In the above equations, $P_f(p_T^\gamma)$ and $P_f(p_T^h, p_T^\gamma)$ are the final-state distribution functions for single-photon and back-to-back photon-hadron production, while $P_i(p_T^j)$ and $P_i(p_T^j, p_T^{j'})$ are the initial distributions for a jet or jet pair to be produced in the medium with the given momenta and species types. The yield per trigger $P(p_T^\gamma|p_T^j,\vec{r}_\perp,\phi)$ is the number of produced photons given an initial jet, which may be decomposed into different contributions,

$$P(p_T^\gamma|p_T^j,\vec{r}_\perp,\phi) = \sum_{\rm src}P(p_T^\gamma,{\rm src}|p_T^j,\vec{r}_\perp,\phi), \quad (14)$$

where the sources include direct photons, fragmentation photons, and jet-medium photons as described in the last section. For the direct photon contribution, the near-side jet is replaced by a direct photon, so the yield per trigger is simply given by $P(p_T^\gamma,{\rm direct}|p_T^j,\vec{r}_\perp,\phi) = \delta(p_T^\gamma - p_T^j)$. The fragmentation photon contribution is related to the medium-modified photon fragmentation function by $P(p_T^\gamma,{\rm frag}|p_T^j,\vec{r}_\perp,\phi) = \tilde{D}_{\gamma/j}(z,\vec{r}_\perp,\phi)/p_T^j$, with $z = p_T^\gamma/p_T^j$. Furthermore, we also need to include the contribution from jet-medium photons, which is achieved by solving Eq. (10), the photon evolution equation, to obtain the yield per trigger $P(p_T^\gamma,{\rm JM}|p_T^j,\vec{r}_\perp,\phi)$. Note that for the case of hadron yield per jet trigger $P(p_T^h|p_T^j,\vec{r}_\perp,\phi)$, we only need to include the fragmentation contribution because we focus on high-p_T hadron production.

For the study of photon-hadron correlations, it is often useful to define the photon-triggered fragmentation function as follows [59,60],

$$D_{AA}(z_T, p_T^\gamma) = p_T^\gamma P_{AA}(p_T^h | p_T^\gamma), \tag{15}$$

with $z_T = p_T^h / p_T^\gamma$. To quantify the effect of the nuclear medium on the photon-hadron correlations, we may also introduce the nuclear modification factor I_{AA}, which is defined as the ratio between $A + A$ and $p + p$ collisions of the photon-triggered fragmentation function,

$$I_{AA}(z_T, p_T^\gamma) = \frac{D_{AA}(z_T, p_T^\gamma)}{D_{pp}(z_T, p_T^\gamma)}. \tag{16}$$

V. RESULTS AT RHIC

In the previous sections, we have outlined the theoretical formalism for calculating jet energy loss, the production of high-p_T hadrons and photons, and photon-hadron correlations. In this section, we apply this methodology to study Au + Au collisions at RHIC, using a $(3+1)$-dimensional relativistic ideal hydrodynamics [20] and compare our results to available experimental measurements.

In Fig. 1 we show our earlier study [29] of the neutral pion R_{AA} in Au + Au collisions at RHIC measured at midrapidity for two different impact parameters, 2.4 and 7.5 fm, compared with the experimental measurements by PHENIX [2] for the most central (0–5%) and midcentral (20–30%) collisions. In the calculation, the strong coupling constant α_s is adjusted in such a way that the experimental measurement of R_{AA} in most central collisions (upper panel) is described. The same value, $\alpha_s = 0.27$, is used throughout the calculation. (There is no additional parameter for the later calculation of high-p_T photon production and photon-hadron correlations.) Figure 1 also compares the relative contributions of induced gluon radiations and elastic collisions to the final R_{AA}. One may find that while the shape does not show a strong sensitivity, the overall magnitude of R_{AA} is sensitive to both radiative and collisional energy loss.

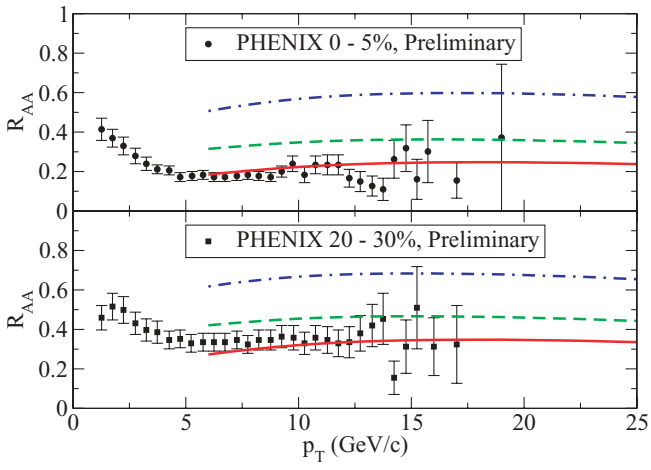

FIG. 1. (Color online) The nuclear modification factor R_{AA} for neutral pions in central and midcentral collisions (from Ref. [29]). The dashed curves account for only induced gluon radiation, the dash-dotted curves for only elastic collisions and the solid curves incorporate both elastic and inelastic energy losses.

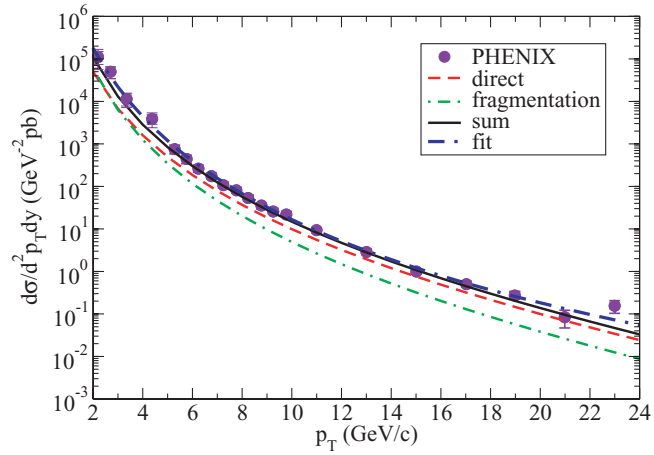

FIG. 2. (Color online) Photon production in $p + p$ collisions compared with PHENIX data [61,62].

Next, we present the results for high-p_T photon production at RHIC. In Fig. 2, the inclusive photon cross section in $p + p$ collisions at $\sqrt{s_{NN}} = 200$ GeV as a function of photon p_T is compared with the experimental measurements by PHENIX [61,62]. The theoretical calculation can nicely describe the experimental data; this serves as the baseline for calculating photon production in Au + Au collisions. Photons from early hard collisions (Compton scatterings and annihilation processes) dominate at high-p_T regimes, while fragmentation photons gain increasing significance as photon p_T decreases. Also shown is a power-law fit to the experimental measurement of total photon yield in $p + p$ collisions at RHIC: $d\sigma/d^2p_T dy = 1.027/(1 + p_T/0.793\,\text{GeV})^{6.873}\text{GeV}^{-2}\text{mb}$. This function is somewhat closer to the low-p_T experimental data, and its usefulness will become clear shortly.

In Fig. 3, the relative contributions from different channels to high-p_T photon production in central Au + Au collisions

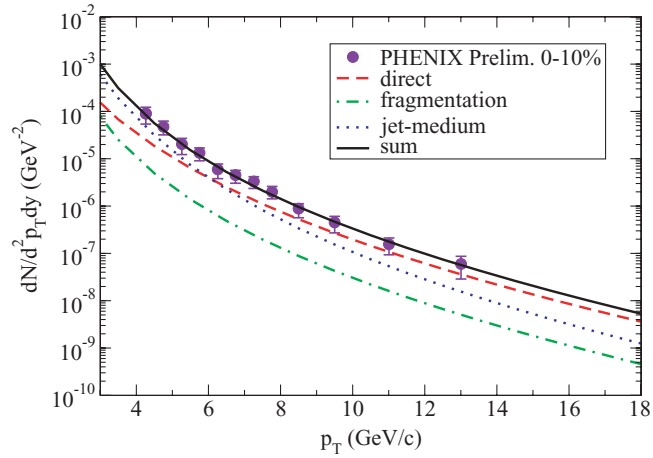

FIG. 3. (Color online) The contributions from different channels to the photon production in Au + Au collisions at RHIC for $b = 2.4$ fm compared with PHENIX data [63].

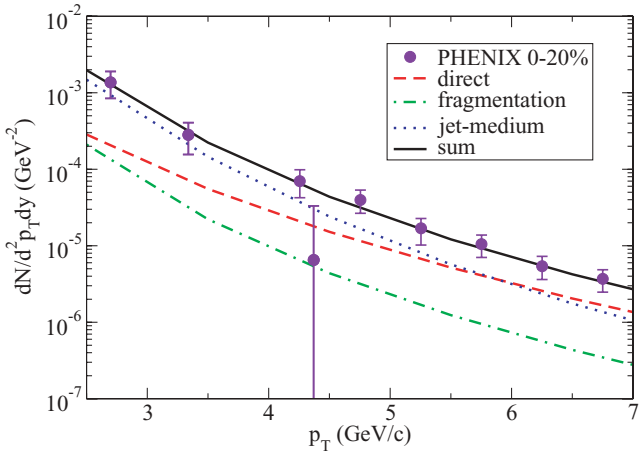

FIG. 4. (Color online) The contributions from different channels to the photon production in Au + Au collisions at RHIC for $b = 4.5$ fm compared with date from the PHENIX Collaboration [62,63].

($b = 2.4$ fm) at RHIC is shown as a function of photon p_T and compared with most central 0–10% PHENIX data [63]. While direct photons dominate the high-p_T regime ($p_T \geqslant 6$ GeV), the presence of jet-medium interaction is a significant contribution to the total photon yield in Au + Au collisions at RHIC, especially in the intermediate-p_T regime ($p_T \approx 3$–5 GeV). This can be more easily seen in Fig. 4, where we compare our calculation of photon production for $b = 4.5$ fm in the intermediate-p_T regime with 0–20% Au + Au collisions data from PHENIX [62,63]. At very low p_T ($p_T \leqslant 2$ GeV), the thermal emissions from partonic and hadronic phases are expected to dominate [64]. This component is excluded in the calculation as we are focusing on the high-p_T regime. Also the assumptions essential for jet-energy loss calculation break down at such low p_T.

To further quantify nuclear medium effects on photon production in Au + Au collisions, we show in Fig. 5 the calculated photon R_{AA} as a function of photon p_T for central Au + Au collisions ($b = 2.4$ fm) at RHIC compared with

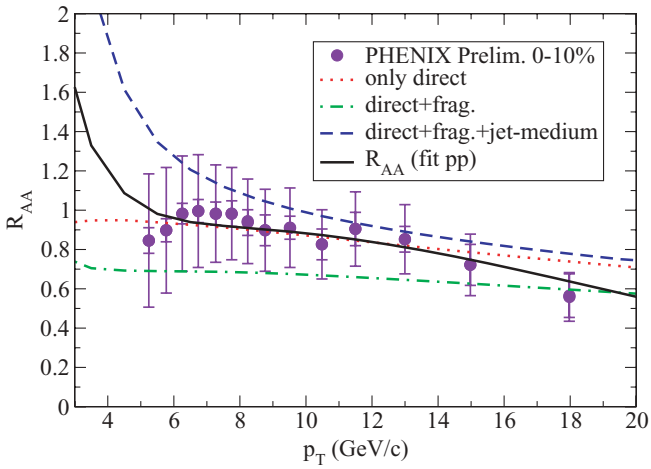

FIG. 5. (Color online) The nuclear modification factor R_{AA} calculated for photons in Au + Au collisions at RHIC for $b = 2.4$ fm compared with PHENIX data with a 0–10% centrality cut [63].

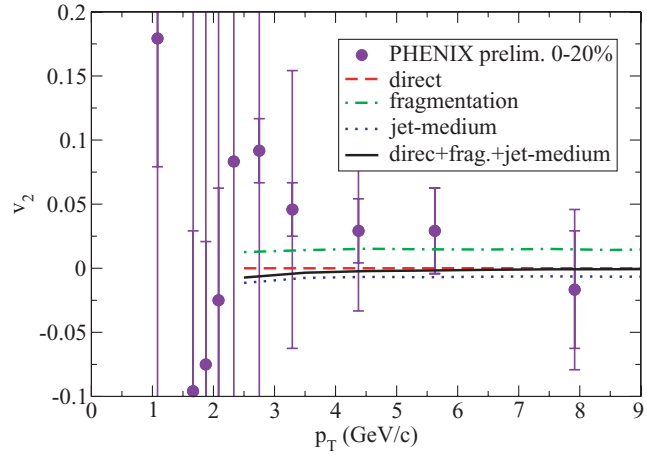

FIG. 6. (Color online) The photon momentum azimuthal asymmetry, v_2, as a function of the photon transverse momentum. The different components are explained in the text, and the data are from Ref. [65].

most 0–10% PHENIX data. The figure shows that R_{AA} can be smaller than 1 even if only direct and fragmentation photons are included in both $p + p$ and Au + Au calculations. As direct photons dominate the total yield (and thus R_{AA}) in the high-p_T regime, the decrease of R_{AA} at high p_T is consistent with an isospin effect. If we include the contribution from fragmentation photons in the calculation, photon R_{AA} gets suppressed because these photons are produced from the fragmentation of the surviving jets with less energies due to the energy loss of jets when they are traversing the thermalized medium. However, the presence of jet-medium interaction in Au + Au collisions (but not in $p + p$ collisions) again enhances R_{AA} if we include them in the total photon yield. It is telling that the sharp rise of R_{AA} at low-p_T originates mainly from the fact that our calculation for $p + p$ collisions is below the data points (see Fig. 2): a better agreement with the data is obtained with the power-law fit to the $p + p$ data used to calculate R_{AA}. The additional QGP sources then manifest themselves in the difference between the solid and the dash-dotted curves in Fig. 5. The sensitivity of R_{AA} to this level of details also makes clear the need for a precise, QCD-based, quantitative understanding of photon data in $p + p$ collisions.

The nucleus-nucleus photon data can also be analyzed in terms of its anisotropy in momentum space, which is characterized by the well-known v_2 coefficient. This data is show in Fig. 6. It is clear that the high centrality cut will cause the momentum anisotropy to be small, and this is indeed what is observed. Moreover, the intrinsically negative v_2 associated with jet-medium photons is drastically reduced in absolute magnitude when combined with the other components whose momentum anisotropy is either zero or positive. Recall that the thermal photons, not included in this calculation, will kick in as the transverse momentum gets lower than $p_T \sim 3$–4 GeV/c, and that their v_2 is positive [34,66]. A combination of isolation and centrality cuts will be needed to clearly isolate the predicted [67] negative contribution [34].

So far, we have just considered single jets and single photons. Now, results for the correlation between back-to-back

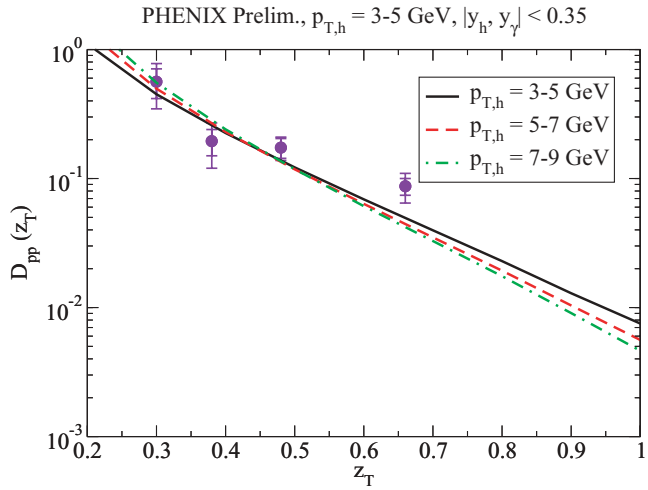

FIG. 7. (Color online) The photon-triggered fragmentation function as a function of momentum fraction z_T in $p + p$ collisions at RHIC.

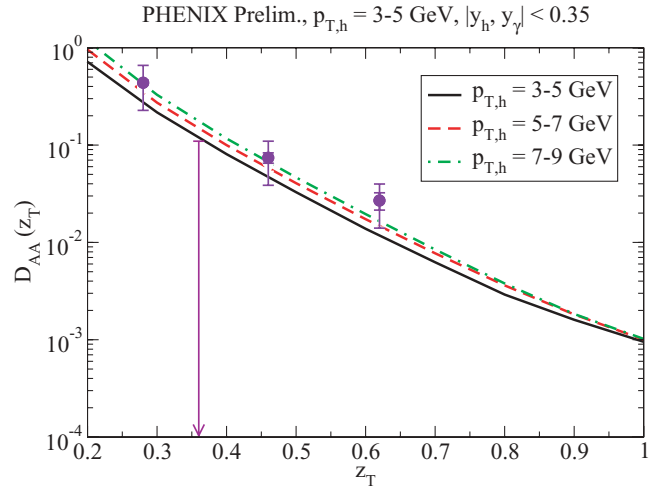

FIG. 8. (Color online) The photon-triggered fragmentation function as a function of momentum fraction z_T in Au + Au collisions at RHIC, with $b = 4.5$ fm.

high-p_T trigger photons and associated hadrons will be discussed. In Fig. 7, the photon-triggered fragmentation function $D_{pp}(z_T)$ in $p + p$ collisions at RHIC is plotted as a function of momentum fraction z_T for three different associated hadron p_T ranges: $p_T^h = 3$–5, 5–7, and 7–9 GeV. The experimental data are taken from PHENIX [68], and we have chosen those data points with highest transverse momentum for associated hadrons ($p_T^h = 3$–5 GeV) such that fragmentation might be dominant for hadron production. We find that the slopes of the photon-triggered fragmentation function $D_{pp}(z_T)$ are slightly different for the three hadron p_T ranges. We may trace this difference back to the different momentum (fraction) dependence of initial parton distribution functions (PDF) for quarks and gluons (a steeper slope for gluon PDF than quark PDF as a function of momentum fraction). As we increase the momenta of initial partons (and therefore Bjorken x) more quarks appear in the initial state, so the relative importance of $q\bar{q} \to g\gamma$ increases compared to $qg \to q\gamma$. As a consequence, the photon-triggered fragmentation function $D_{pp}(z_T)$, which is an average over quark and gluon fragmentation functions weighted with their fractions, will become steeper, because the gluon fragmentation function is steeper than that for quarks.

In Fig. 8, we show our results for the photon-triggered fragmentation function $D_{AA}(z_T)$ in midcentral Au + Au collisions ($b = 4.5$ fm) as a function of momentum fraction z_T, compared with 0–20% data from PHENIX [68]. The dependence of $D_{AA}(z_T)$ on associated hadron p_T is similar to $D_{pp}(z_T)$ in the low-z_T regime because the associated hadrons are mostly produced from those jets triggered by direct photons (see Fig. 13). However, this difference tends to decrease at high z_T due to the presence of jet-medium interaction in Au + Au collisions. Because jet-plasma photons and fragmentation photons assume more significance to photon production at lower p_T (see Fig. 4), a larger enhancement is obtained for smaller associated hadron p_T.

To further quantify the nuclear medium effect on the photon-triggered hadron production, we may take the ratio of D_{AA} to D_{pp} and calculate the nuclear modification factor I_{AA} for photon-triggered hadron production. The result is shown in Fig. 9 and compared with experimental measurement by PHENIX. At low z_T, I_{AA} falls with increasing z_T due to the dominance of direct photons, but it flattens out at higher z_T due to the effect of jet-medium photons and fragmentation photons (see Fig. 13).

Also, we compare our calculation with STAR measurements [69]. In Fig. 10, we show the photon-triggered fragmentation function $D_{AA}(z_T)$ as a function of momentum fraction z_T in central Au + Au collisions ($b = 2.4$ GeV) at RHIC. The trigger photon momenta have been chosen to be $p_T^\gamma = 8$–16 GeV. The theoretical curve of photon-triggered fragmentation function $D_{AA}(z_T)$ in central Au + Au collisions agrees with experimental data quite well. The data for peripheral (40–80%) Au + Au collisions are also shown in the figure for the interest of comparing with the $p + p$ calculation.

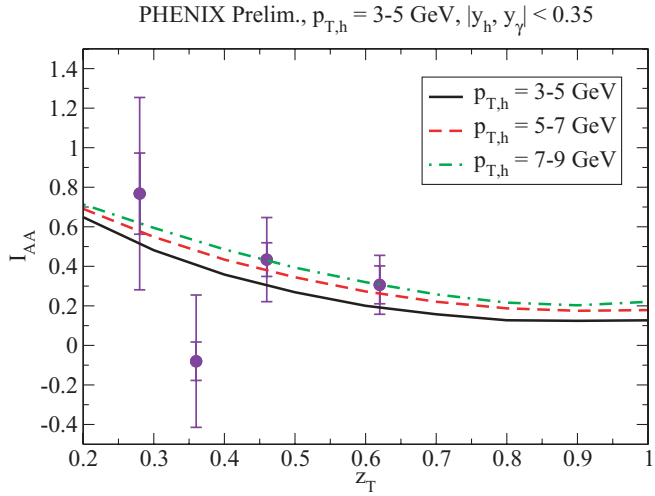

FIG. 9. (Color online) Photon-triggered I_{AA} as a function of momentum fraction z_T in Au + Au collisions at RHIC, with $b = 4.5$ fm.

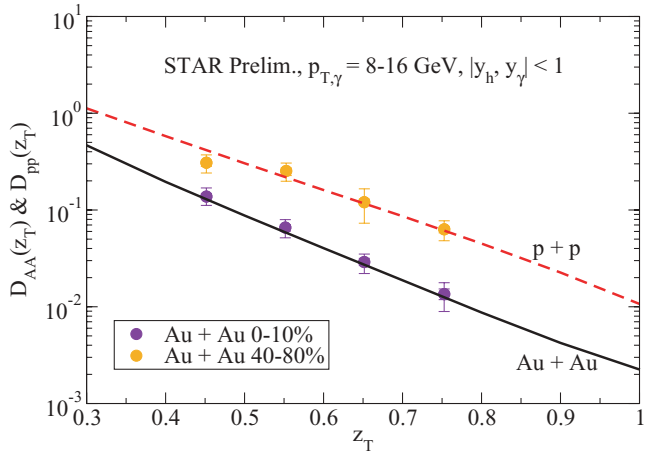

FIG. 10. (Color online) The photon-triggered fragmentation functions as a function of momentum fraction z_T in central Au + Au collisions and $p + p$ collisions (peripheral Au + Au collisions) at RHIC.

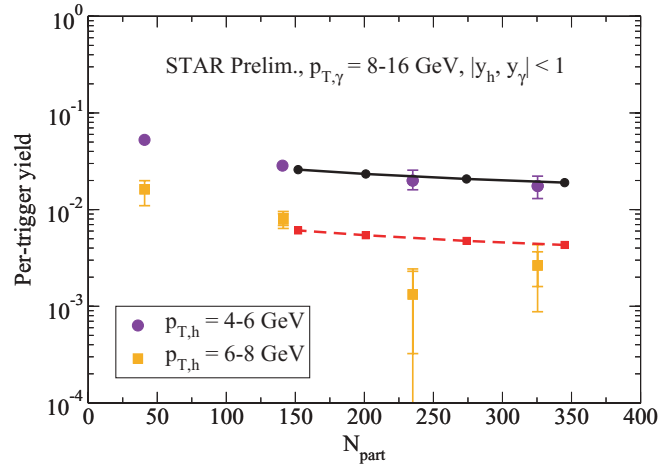

FIG. 12. (Color online) The per-trigger yield for photon-tagged hadrons in Au + Au collisions at RHIC as a function of centrality. The four points in each theoretical curve correspond to four impact parameters, 2.4, 4.5, 6.3, and 7.5 fm.

For completeness, the nuclear modification factor I_{AA} for photon-triggered hadron production is plotted in Fig. 11 as a function of momentum fraction z_T and hadron momentum p_T^h. While I_{AA} as a function of z_T is similar to Fig. 9, I_{AA} is a rather flat function of p_T^h because fixing p_T^h with a wide range of p_T^γ is actually an average over a variety of z_T.

We also study the medium-size dependence of photon-hadron correlations by calculating the photon-triggered hadron production in noncentral collisions. By integrating over the transverse momenta of both trigger photons and associated hadrons, we study the centrality dependence of the per-trigger yield of photon-triggered hadrons in Au + Au collisions at RHIC. This result is plotted in Fig. 12, where the experimental measurements are from STAR [69]. In the calculation, we have chosen four different impact parameters, 2.4, 4.5, 6.3, and 7.5 fm, which correspond to four points in each theoretical curve. We do not perform the calculation for very peripheral collisions because the assumption of a thermalized medium essential for a hydrodynamical treatment is no longer fulfilled. Again, the trigger photon p_T has been chosen to be $p_T^\gamma = 8$–16 GeV, and two different hadron p_T ranges ($p_T^h =$ 4–6 GeV and 6–8 GeV) are studied. We find that the centrality dependence of per-trigger yield from the calculation is also consistent with current experimental measurements.

In the above results, we have taken into account all possible sources of high-p_T photon production. It would be interesting to study how different sources of photons contribute the final photon-triggered hadron production. To address this issue, we may decompose the per-trigger yield of hadrons into different parts, each associated with a specific photon source,

$$P\left(p_T^h \middle| p_T^\gamma\right) = \sum_{\text{src}} P\left(p_T^h, \text{src} \middle| p_T^\gamma\right), \tag{17}$$

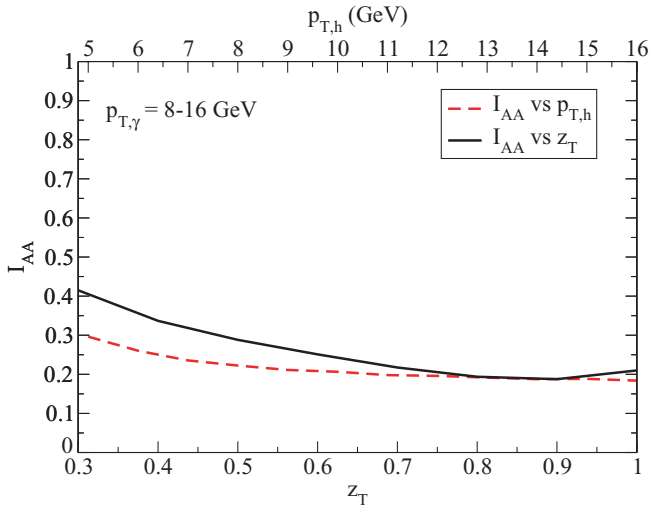

FIG. 11. (Color online) Photon-triggered I_{AA} for hadrons as a function of hadron momentum p_T or momentum fraction z_T in Au + Au collisions at RHIC, with $b = 2.4$ fm.

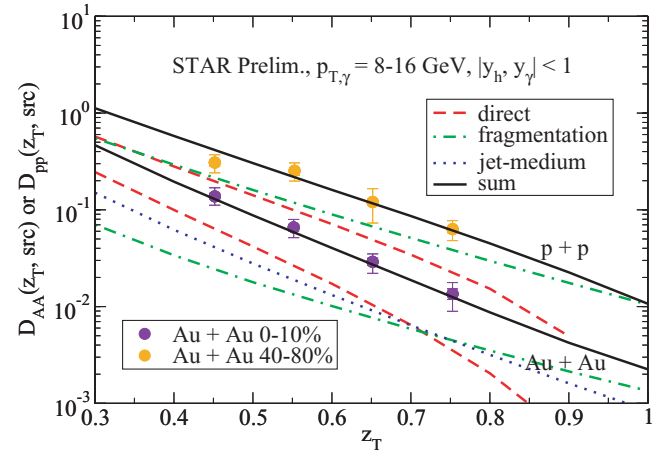

FIG. 13. (Color online) The contributions from different photon channels to the photon-triggered fragmentation function in $p + p$ collisions and Au + Au collisions at RHIC.

where $P(p_T^h, \text{src}|p_T^\gamma) = P(p_T^h, p_T^\gamma, \text{src})/P(p_T^\gamma)$. A similar decomposition may be performed for photon-triggered fragmentation functions. In Fig. 13, we show the relative contributions from different photon sources to the photon-triggered fragmentation function $D(z_T, p_T^\gamma)$ in both $p + p$ collisions and central Au + Au collisions ($b = 2.4$ fm) if we trigger on a photon on the near side. We find that about half of the away-side hadrons at relatively small z_T are produced from those jets tagged by direct photons, while at higher z_T, a large amount of away-side hadrons come from those jets tagged by jet-medium photons and fragmentation photons. Especially, close to $z_T = 1$, where the associated hadrons have almost the same amount of transverse momentum as the trigger photon, the away-side hadron production is dominated by those jets tagged by fragmentation photons. Therefore, it would be interesting to extend the experimental data to higher z_T (and to high p_T^h such that fragmentation dominates hadron production), where jet-medium interaction and fragmentation make a significant contribution to photon-hadron correlations.

VI. CONCLUSIONS

In this work, we have studied jet energy loss and photon production at high p_T together in the same framework, with additional information provided by photon-hadron correlations. The energy loss of hard jets traversing the hot and dense medium is computed by a consistent incorporation of both induced gluon radiation and elastic collisions. The production of high-p_T photons is obtained by taking into account a complete set of photon-production channels. Numerical results have been presented and compared with experimental measurements by employing a fully $(3 + 1)$-dimensional hydrodynamical evolution model for the description of the thermalized medium created at RHIC.

Our results illustrate that the magnitude of jet quenching in relativistic nuclear collisions is sensitive to the inclusion of both radiative and collisional energy loss. It is also found that the interaction between jets and the thermalized medium makes a significant contribution to the total photon production at RHIC. Therefore, it is important to incorporate all sources of hard photons for a full understanding of the correlations between back-to-back hard photons and hadrons. In summary, our study provides the groundwork to experimentally test our understanding of the jet-medium interaction and further extract detailed information about the hot and dense medium created at RHIC.

ACKNOWLEDGMENTS

We are indebted to C. Nonaka and S. Bass for providing their hydrodynamical evolution calculation [20]. We thank T. Renk and M. Tannenbaum for interesting discussions and A. M. Hamed and B. Schenke for interesting discussions and a critical reading of this manuscript. This work was supported in part by the US Department of Energy under Grant DE-FG02-01ER41190 and in part by the Natural Sciences and Engineering Research Council of Canada.

[1] K. Adcox *et al.* (PHENIX Collaboration), Phys. Rev. Lett. **88**, 022301 (2002).
[2] C. Adler *et al.* (STAR Collaboration), Phys. Rev. Lett. **89**, 202301 (2002).
[3] M. Gyulassy and X.-N. Wang, Nucl. Phys. **B420**, 583 (1994).
[4] A. B. Migdal, Phys. Rev. **103**, 1811 (1956).
[5] R. Baier, Y. L. Dokshitzer, A. H. Mueller, S. Peigne, and D. Schiff, Nucl. Phys. **B483**, 291 (1997).
[6] A. Kovner and U. A. Wiedemann (2003), arXiv:hep-ph/0304151.
[7] B. G. Zakharov, JETP Lett. **63**, 952 (1996).
[8] M. Gyulassy, P. Levai, and I. Vitev, Nucl. Phys. **B594**, 371 (2001).
[9] X.-N. Wang and X.-F. Guo, Nucl. Phys. **A696**, 788 (2001).
[10] B.-W. Zhang and X.-N. Wang, Nucl. Phys. **A720**, 429 (2003).
[11] A. Majumder, E. Wang, and X.-N. Wang, Phys. Rev. Lett. **99**, 152301 (2007).
[12] A. Majumder and B. Muller, Phys. Rev. C **77**, 054903 (2008).
[13] P. Arnold, G. D. Moore, and L. G. Yaffe, J. High Energy Phys. 12 (2001) 009.
[14] P. Arnold, G. D. Moore, and L. G. Yaffe, J. High Energy Phys. 11 (2001) 057.
[15] P. Arnold, G. D. Moore, and L. G. Yaffe, J. High Energy Phys. 06 (2002) 030.
[16] G.-Y. Qin, J. Ruppert, S. Turbide, C. Gale, C. Nonaka, and S. A. Bass, Phys. Rev. C **76**, 064907 (2007).
[17] T. Renk, J. Ruppert, C. Nonaka, and S. A. Bass, Phys. Rev. C **75**, 031902(R) (2007).
[18] A. Majumder, C. Nonaka, and S. A. Bass, Phys. Rev. C **76**, 041902(R) (2007).
[19] S. A. Bass *et al.*, Phys. Rev. C **79**, 024901 (2009).
[20] C. Nonaka and S. A. Bass, Phys. Rev. C **75**, 014902 (2007).
[21] J. D. Bjorken, FERMILAB-PUB-82-059-THY.
[22] M. G. Mustafa and M. H. Thoma, Acta Phys. Hung. **A22**, 93 (2005).
[23] M. G. Mustafa, Phys. Rev. C **72**, 014905 (2005).
[24] A. Adil, M. Gyulassy, W. A. Horowitz, and S. Wicks, Phys. Rev. C **75**, 044906 (2007).
[25] S. Wicks and M. Gyulassy, J. Phys. G **34**, S989 (2007).
[26] B. G. Zakharov, JETP Lett. **86**, 444 (2007).
[27] T. Renk, Phys. Rev. C **76**, 064905 (2007).
[28] A. Majumder, Phys. Rev. C **80**, 031902 (2009).
[29] G.-Y. Qin, J. Ruppert, C. Gale, S. Jeon, G. D. Moore, and M. G. Mustafa, Phys. Rev. Lett. **100**, 072301 (2008).
[30] B. Schenke, C. Gale, and G.-Y. Qin, Phys. Rev. C **79**, 054908 (2009).
[31] C. Gale (2009), arXiv:0904.2184.
[32] R. J. Fries, B. Muller, and D. K. Srivastava, Phys. Rev. Lett. **90**, 132301 (2003).
[33] S. Turbide, C. Gale, S. Jeon, and G. D. Moore, Phys. Rev. C **72**, 014906 (2005).
[34] S. Turbide, C. Gale, E. Frodermann, and U. Heinz, Phys. Rev. C **77**, 024909 (2008).
[35] T. Renk, Phys. Rev. C **74**, 034906 (2006).
[36] A. Majumder, Phys. Rev. C **75**, 021901(R) (2007).
[37] T. Renk and K. J. Eskola, Phys. Rev. C **75**, 054910 (2007).

[38] X.-N. Wang, Z. Huang, and I. Sarcevic, Phys. Rev. Lett. **77**, 231 (1996).
[39] X.-N. Wang and Z. Huang, Phys. Rev. C **55**, 3047 (1997).
[40] K. Filimonov, Acta Phys. Hung. **A25**, 363 (2006).
[41] F. Arleo, J. Phys. G **34**, S1037 (2007).
[42] H. Zhang, J. F. Owens, E. Wang, and X.-N. Wang, Phys. Rev. Lett. **103**, 032302 (2009).
[43] S. Jeon and G. D. Moore, Phys. Rev. C **71**, 034901 (2005).
[44] G.-Y. Qin *et al.* (2008), arXiv:0805.4594.
[45] J. F. Owens, Rev. Mod. Phys. **59**, 465 (1987).
[46] H. L. Lai *et al.*, Eur. Phys. J. C **12**, 375 (2000).
[47] K. J. Eskola, V. J. Kolhinen, and C. A. Salgado, Eur. Phys. J. C **9**, 61 (1999).
[48] K. J. Eskola, H. Honkanen, H. Niemi, P. V. Ruuskanen, and S. S. Rasanen, Phys. Rev. C **72**, 044904 (2005).
[49] B. A. Kniehl, G. Kramer, and B. Potter, Nucl. Phys. **B582**, 514 (2000).
[50] C. W. De Jager, H. De Vries, and C. De Vries, At. Data Nucl. Data Tables **14**, 479 (1974).
[51] P. Aurenche, R. Baier, M. Fontannaz, and D. Schiff, Nucl. Phys. **B297**, 661 (1988).
[52] F. Aversa, P. Chiappetta, M. Greco, and J. P. Guillet, Nucl. Phys. **B327**, 105 (1989).
[53] P. Aurenche *et al.*, Eur. Phys. J. C **9**, 107 (1999).
[54] L. Bourhis, M. Fontannaz, and J. P. Guillet, Eur. Phys. J. C **2**, 529 (1998).
[55] G. Y. Qin, J. Ruppert, C. Gale, S. Jeon, and G. D. Moore (2008), arXiv:0809.2030.
[56] J. I. Kapusta, P. Lichard, and D. Seibert, Phys. Rev. D **44**, 2774 (1991).
[57] R. Baier, H. Nakkagawa, A. Niegawa, and K. Redlich, Z. Phys. C **53**, 433 (1992).
[58] A. Adare *et al.* (PHENIX Collaboration), Phys. Rev. C **78**, 014901 (2008).
[59] X.-N. Wang, Phys. Lett. **B595**, 165 (2004).
[60] X.-N. Wang, Phys. Lett. **B579**, 299 (2004).
[61] S. S. Adler *et al.* (PHENIX Collaboration), Phys. Rev. Lett. **98**, 012002 (2007).
[62] A. Adare *et al.* (PHENIX Collaboration) (2008), arXiv:0804.4168.
[63] T. Isobe (PHENIX Collaboration), J. Phys. G **34**, S1015 (2007).
[64] S. Turbide, R. Rapp, and C. Gale, Phys. Rev. C **69**, 014903 (2004).
[65] K. Miki (PHENIX Collaboration), J. Phys. G **35**, 104122 (2008).
[66] R. Chatterjee, E. S. Frodermann, U. W. Heinz, and D. K. Srivastava, Phys. Rev. Lett. **96**, 202302 (2006).
[67] S. Turbide, C. Gale, and R. J. Fries, Phys. Rev. Lett. **96**, 032303 (2006).
[68] A. Adare *et al.* (PHENIX Collaboration), Phys. Rev. C **80**, 024908 (2009).
[69] A. M. Hamed (STAR Collaboration), J. Phys. G **35**, 104120 (2008).